

Forced Convective Heat Transfer Enhancement in a Tube with its Core Partially Filled with a Porous Medium

C. Yang^{1,2}, W. Liu¹ and A. Nakayama^{*2}

¹School of Energy and Power Engineering, Huazhong University of Science and Technology, Wuhan, Hubei 430074, P.R. China

²Department of Mechanical Engineering, Shizuoka University, 3-5-1 Johoku, Hamamatsu, 432-8561, Japan

Abstract: Forced convection in a tube with its core partially filled with a porous medium is treated both analytically and numerically to find its high heat transfer performance. Assuming a fully developed flow subject to a constant heat flux, both friction factor and Nusselt number are presented explicitly as functions of the Reynolds number, Darcy number and porous core diameter ratio. Partial filling of the porous medium in the core region leads the fluid particles close to the wall, resulting an increase in the heat transfer coefficient. Extensive filling, however, tends to block the fluid particles channeling through the small gap formed between the wall and the porous core interface. Consequently, there exists the optimal porous core diameter ratio as a function of the Darcy number, which yields the maximum heat transfer coefficient.

Keywords: Heat transfer enhancement, porous media, circular tube flow, forced convection.

INTRODUCTION

A considerable number of investigations on forced convection in a tube fully or partially filled with a porous medium were reported in view of its possible potential in enhancing heat transfer performance [1-3]. Obviously a partial filling has the advantage of a comparable increase in the heat transfer performance at expense of only a smaller increase in the pressure drop. Some analytical expressions associated with hydraulic and thermal characteristics were obtained for fully developed channel flows with various thermal boundary conditions such as constant wall temperature and constant wall heat flux conditions.

Al-Nimr and Alkam [4] numerically investigated forced convection in a concentric annulus partially filled with a porous medium and reported an increase of 12 times in the heat transfer coefficient as compared with the annulus without a porous medium. Al-Nimr and Alkam [5] also proposed to place porous substrates on both sides of the inner cylinders of conventional concentric tube heat exchanger to achieve higher heat transfer performance with an only moderate increase in the pumping power. An extensive numerical investigation was conducted by Mohamad [6] to confirm possible heat transfer augmentation for thermally developing flows in a pipe with its core partially filled with a porous medium. He found that partially filling the channel with porous substrates lead to reduction of the thermal entrance length and that an optimum thickness of about 60% of the channel height results in a substantial increase in heat transfer at the expense of a reasonable pressure drop. Pavel and Mohamad [7] conducted an experimental investigation to elucidate the effect of a

metallic porous matrix, inserted in a pipe, on the rate of heat transfer and concluded that higher heat transfer rates are possible when using porous inserts at expense of a reasonable pressure drop. Liu *et al.* [8] carried out a series of numerical computations for laminar forced convection in a tube with its core partially filled with a porous medium. They used the momentum equation proposed by Vafai and Tien [9] to cover both clear fluid layer and porous core region, treating the clear fluid core region as a special kind of porous medium with unit porosity and infinitely large permeability. Upon changing the ratio of the porous medium radius to the tube radius, they found a tremendous heat transfer enhancement is possible when the ratio is close to unity.

However, no quantitative relationships among controlling parameters such as the friction factor, Nusselt number, Darcy number and radius ratio have been presented explicitly in these previous investigations. In this study, we shall revisit the problem of forced convection in a tube with its core partially filled with a porous medium and attack it both analytically and numerically so as to elucidate the heat transfer augmentation mechanism and the corresponding optimum conditions to achieve high heat transfer performance in such conduits partially filled with a porous medium.

MATHEMATICAL MODEL AND GOVERNING EQUATIONS

A mathematical model in consideration is shown in Fig. (1), in which a circular tube of inner diameter d is filled partially with a porous medium of diameter d_i . It is assumed that the tube wall is heated to provide a uniform heat flux q_w and that the tube is long enough for both velocity and temperature fields to be fully developed.

*Address correspondence to this author at the Department of Mechanical Engineering, Shizuoka University, 3-5-1 Johoku, Hamamatsu, 432-8561 Japan; E-mail: tmanaka@ipc.shizuoka.ac.jp

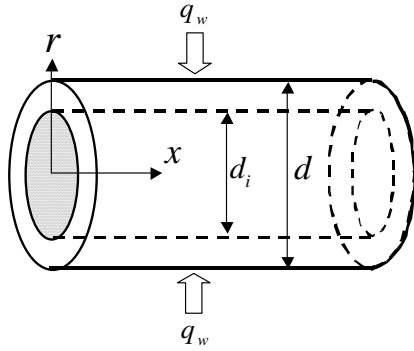


Fig. (1). Tube with its core partially filled with a porous medium.

The governing equations for the case of steady-state fully developed flow under the constant heat flux condition are given by:

Fluid region $d_i/2 \leq r \leq d/2$:

$$-\frac{dp}{dx} + \frac{\mu_f}{r} \frac{d}{dr} \left(r \frac{du}{dr} \right) = 0 \quad (1)$$

$$\rho_f c_{pf} u \frac{\partial T}{\partial x} = \frac{k_f}{r} \frac{\partial}{\partial r} \left(r \frac{\partial T}{\partial r} \right) \quad (2)$$

Porous region $0 \leq r \leq d_i/2$:

$$-\frac{dp}{dx} + \frac{\mu_f}{\varepsilon r} \frac{d}{dr} \left(r \frac{du}{dr} \right) - \frac{\mu_f}{K} u = 0 \quad (3)$$

$$\rho_f c_{pf} u \frac{\partial T}{\partial x} = \frac{k_e}{r} \frac{\partial}{\partial r} \left(r \frac{\partial T}{\partial r} \right) \quad (4)$$

where Brinkman-extended Darcy's law [9] is introduced for the porous core region whose porosity, permeability and effective thermal conductivity are denoted by ε , K and k_e , respectively. Note that the axial velocity u in Equations (3) and (4) corresponds to the Darcian velocity, while the physical properties of the fluid are indicated by the subscript f . Referring to Fig. (2) showing typical velocity and temperature profiles, we may set the boundary conditions as follows:

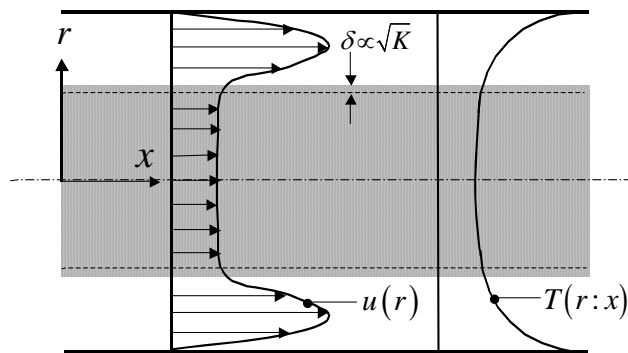


Fig. (2). Velocity and temperature profiles.

For $r = 0$:

$$\frac{du}{dr} = 0, \quad \frac{\partial T}{\partial r} = 0 \quad (5a, b)$$

For $r = d/2$:

$$u = 0, \quad k_f \frac{\partial T}{\partial r} = q_w \quad (6a, b)$$

whereas the interfacial compatibility conditions at $r = d_i/2$ are given by:

$$u|_{(r-d_i/2) \rightarrow -0} = u|_{(r-d_i/2) \rightarrow +0}, \quad \frac{\mu_f}{\varepsilon} \frac{\partial u}{\partial r}|_{(r-d_i/2) \rightarrow -0} = \mu_f \frac{\partial u}{\partial r}|_{(r-d_i/2) \rightarrow +0} \quad (7a, b)$$

$$T|_{(r-d_i/2) \rightarrow -0} = T|_{(r-d_i/2) \rightarrow +0}, \quad k_e \frac{\partial T}{\partial r}|_{(r-d_i/2) \rightarrow -0} = k_f \frac{\partial T}{\partial r}|_{(r-d_i/2) \rightarrow +0} \quad (8a, b)$$

The foregoing set of equations can easily be solved numerically using any one of standard numerical schemes such as SIMPLE [10, 11], exploiting periodic boundary conditions for a finite tube length [12]. Such numerical results will be presented later along with the analytical results based on Darcy's law.

VELOCITY FIELD BASED ON DARCY'S LAW

As indicated in Fig. (2), the Brinkman effects on the velocity are appreciable only within a thin layer of the order $\delta \propto \sqrt{K}$. Therefore, in our analytical treatment, we may drop the second LHS term of Equation (3), which then reduces to Darcy's law such that:

$$u = -\frac{K}{\mu} \frac{dp}{dx} \equiv u_i = \text{const. for } 0 \leq r \leq d_i/2 \quad (9)$$

Subsequently, the velocity profile within the fluid region may readily be determined by integrating Equation (1) as:

$$u = 2u_i \left[\frac{1-\eta^2}{32Da} + \left(1 - \frac{1-R_p^2}{16Da} \right) \frac{\ln \eta}{2 \ln R_p} \right], \quad \text{for } R_p \leq \eta \leq 1 \quad (10)$$

where the dimensionless radial coordinate $\eta = r/(d/2)$ is introduced with the porous core diameter ratio $R_p = d_i/d$ and the Darcy number $Da = K/d^2$. Naturally, Equation (10) satisfies the no-slip condition given by Equation (6a) and the matching condition (7a), namely, $u = u_i$ at $r = d_i/2$.

The interfacial velocity u_i is related to the bulk mean velocity $u_b = \dot{m}/(\rho_f \pi d^2/4)$ in the tube as:

$$\frac{u_i}{u_b} = \frac{1}{\frac{1-R_p^4}{32Da} - \left(1 - \frac{1-R_p^2}{16Da} \right) \frac{1-R_p^2}{2 \ln R_p}} \quad (11)$$

In Fig. (3), the approximate velocity profile given by Equations (9) and (10) along with (11) is compared against the exact one obtained from numerically solving Equations (1) and (3) with the boundary and compatibility conditions

(5a), (6a), (7a) and (7b), for the case of $\varepsilon=0.9$, $Da=10^{-4}$ and $R_p=0.7$. Fairly good agreement can be seen between these two profiles. This indicates that the velocity profile based on Darcy's law is a reasonable approximation for comparatively low permeability cases.

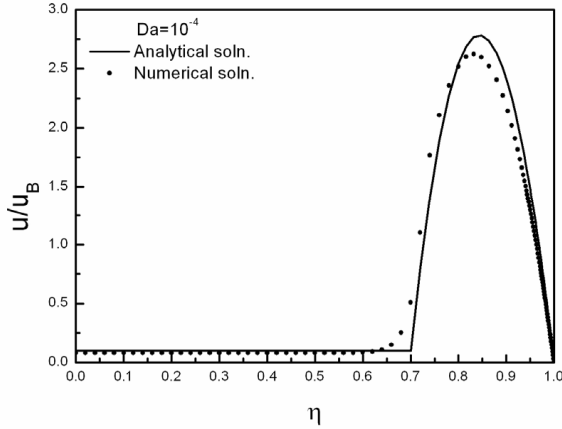


Fig. (3). Fully developed velocity profiles in a tube.

For a given set of Reynolds number $Re_d = u_B d / \nu$ and R_p , the friction factor λ_f may readily be obtained as:

$$\lambda_f \equiv -\frac{2d}{\rho u_B^2} \frac{dp}{dx} = \frac{64}{Re_d \left(1 - R_p^4 - \left(32Da - 2(1 - R_p^2) \right) \frac{1 - R_p^2}{2 \ln R_p} \right)} \quad (12)$$

which reduces $\lambda_f \rightarrow 64 / Re_d$ for $R_p \rightarrow 0$. The effects of R_p on the friction factor are presented in Fig. (4) in terms of the parameter $\lambda_f Re_d / 64$, which may be taken as the pumping power ratio for the case of equal mass flow rate \dot{m} . Naturally, the pumping power increases drastically as $R_p \rightarrow 1$

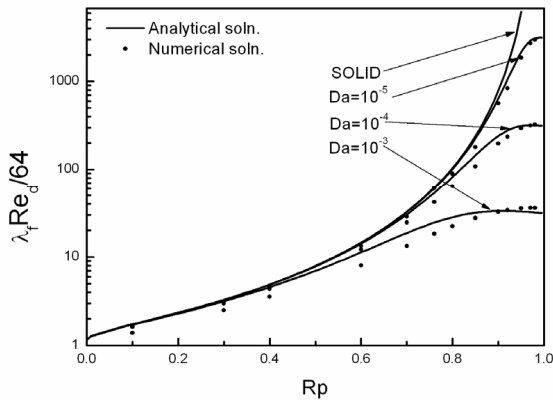


Fig. (4). The effects of R_p on the friction factor λ_f .

TEMPERATURE FIELD AND NUSSELT NUMBER

Having established the velocity field, we shall seek the temperature field and the corresponding Nusselt number. The energy balance for the case of constant heat flux readily gives us:

$$\left(\frac{\pi d^2}{4} \right) \rho_f c_{pf} u_B \frac{dT_B}{dx} = (\pi d) q_w \quad (13)$$

where T_B is the bulk mean temperature. Since $dT_B / dx = \partial T / \partial x$, the Equations (2) and (4) can be rewritten as follows:

$$\left(\frac{4q_w}{d} \right) \left(\frac{u}{u_B} \right) = \frac{k_f}{r} \frac{\partial}{\partial r} \left(r \frac{\partial T}{\partial r} \right) \text{ for } d_i / 2 \leq r \leq d / 2 \quad (14)$$

and

$$\left(\frac{4q_w}{d} \right) \left(\frac{u_i}{u_B} \right) = \frac{k_e}{r} \frac{\partial}{\partial r} \left(r \frac{\partial T}{\partial r} \right) \text{ for } 0 \leq r \leq d_i / 2 \quad (15)$$

We may solve the second order differential equation (14) along with Equation (10) to find the temperature profile within the fluid layer. However, the velocity profile as given by Equation (10) is fairly complex so that a procedure to find the temperature profile and the corresponding bulk temperature is quite formidable. Thus, we shall appeal to an approximate procedure, by integrating (14) for the fluid region as:

$$\left(\frac{\pi q_w}{d} \right) \left(\frac{u_B d^2 - u_i d_i^2}{u_B} \right) = (\pi d) k_f \frac{\partial T}{\partial r} \Big|_{r=d/2} - (\pi d_i) k_f \frac{\partial T}{\partial r} \Big|_{r=d_i/2} \quad (16)$$

which, together with Equation (6b), reduces to:

$$k_f \frac{\partial T}{\partial r} \Big|_{r=d/2} = q_w R_p \left(\frac{u_i}{u_B} \right) \quad (17)$$

We also note writing Equation (14) at the wall as:

$$k_f \left(\frac{\partial^2 T}{\partial r^2} + \frac{1}{r} \frac{\partial T}{\partial r} \right) \Big|_{r=d/2} = 0 \quad (18)$$

Therefore, we expect the temperature profile prevailing within the fluid region to satisfy Equations (17), (18) and (6b). One of the simplest profiles satisfying these conditions would be as follows:

$$\frac{k_f (T - T_w)}{q_w d} = -\frac{3 - 4\eta + \eta^2}{4} + \frac{2 - \left(\frac{u_i}{u_B} \right) R_p - R_p}{6(1 - R_p)^2} (1 - \eta)^3 \text{ for } R_p \leq \eta \leq 1 \quad (19)$$

The temperature profile for the porous core region may readily be obtained by integrating Equation (15) with the boundary condition (5b) and the matching condition (8a) as:

$$\frac{k_f (T - T_w)}{q_w d} = -\frac{5 - 6R_p + R_p^2 + 2(1 - R_p) R_p \left(\frac{u_i}{u_B} \right)}{12} + \left(\frac{k_f}{k_e} \right) \left(\frac{u_i}{u_B} \right) \frac{\eta^2 - R_p^2}{4} \text{ for } 0 \leq \eta \leq R_p \quad (20)$$

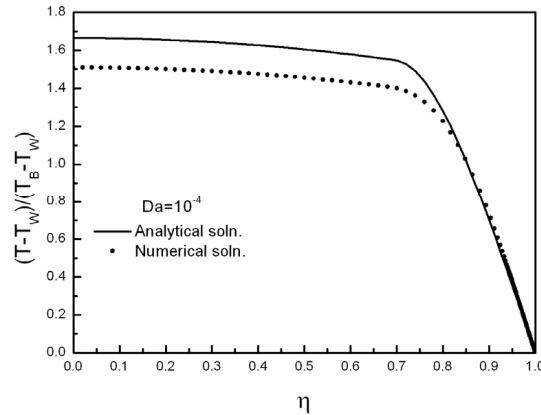


Fig. (5). Fully developed temperature profiles in a tube.

Note that Equations (19) and (20) automatically satisfy the matching condition (8b).

The temperature profile is generated using the foregoing Equations (19) and (20) along with (11) for the case of $\varepsilon=0.9$, $Da=10^{-4}$ and $R_p=0.7$ and plotted in Fig. (5) to compare with the exact numerical solution based on Brinkman extended Darcy’s law. Despite of the difference in the temperature in the core region, two profiles are generally in good agreement.

The corresponding Nusselt number of our primary concern may be obtained following the definition of the bulk mean temperature as:

$$\begin{aligned} \frac{1}{Nu_d} &= -\frac{k_f(T_B - T_w)}{q_w d} = -\frac{4}{\pi d^2} \int_0^{d/2} 2\pi r \left(\frac{u}{u_B}\right) \frac{k_f(T - T_w)}{q_w d} dr \\ &= -2 \left(\frac{u_i}{u_B}\right) \int_0^{R_p} \eta \left[\frac{5 - 6R_p + R_p^2 + 2(1 - R_p)R_p \left(\frac{u_i}{u_B}\right)}{12} + \left(\frac{k_f}{k_e}\right) \left(\frac{u_i}{u_B}\right) \frac{\eta^2 - R_p^2}{4} \right] d\eta \\ &\quad - 2 \left(\frac{u_i}{u_B}\right) \int_{R_p}^1 2\eta \left[\frac{1 - \eta^2}{32Da} + \left(1 - \frac{1 - R_p^2}{16Da}\right) \frac{\ln \eta}{2 \ln R_p} \right] \left[-\frac{3 - 4\eta + \eta^2}{4} + \frac{2 - \left(\frac{u_i}{u_B}\right)R_p - R_p}{6(1 - R_p)^2} (1 - \eta)^3 \right] d\eta \end{aligned} \tag{21}$$

Hence, we have:

$$\begin{aligned} \frac{1}{Nu_d} &= \left(\frac{u_i}{u_B}\right) \left[\left(\frac{3 - 4R_p + R_p^2}{4} - \frac{2 - (u_i/u_B)R_p - R_p}{6} (1 - R_p) + \frac{(u_i/u_B)}{8(k_e/k_f)} R_p^2 \right) R_p^2 \right. \\ &\quad \left. + \frac{1}{32Da} \left(\frac{3}{2}(1 - R_p^2) - \frac{4}{3}(1 - R_p^3) - \frac{1}{2}(1 - R_p^4) + \frac{4}{5}(1 - R_p^5) - \frac{1}{6}(1 - R_p^6) \right) \right. \\ &\quad \left. + \frac{2 - (u_i/u_B)R_p - R_p}{48Da(1 - R_p)^2} \left(-\frac{1 - R_p^2}{2} + 1 - R_p^3 - \frac{1 - R_p^4}{2} - \frac{2}{5}(1 - R_p^5) + \frac{1 - R_p^6}{2} - \frac{1 - R_p^7}{7} \right) \right. \\ &\quad \left. + \frac{1}{2 \ln R_p} \left(1 - \frac{1 - R_p^2}{16Da} \right) \left(-\frac{3}{2} R_p^2 \ln R_p - \frac{3}{4}(1 - R_p^2) + \frac{4}{3} R_p^3 \ln R_p + \frac{4}{9}(1 - R_p^3) - \frac{1}{4} R_p^4 \ln R_p - \frac{1 - R_p^4}{16} \right) \right. \\ &\quad \left. + \frac{2 - (u_i/u_B)R_p - R_p}{3(1 - R_p)^2 \ln R_p} \left(1 - \frac{1 - R_p^2}{16Da} \right) \left(\frac{1}{2} R_p^2 \ln R_p + \frac{1 - R_p^2}{4} - R_p^3 \ln R_p - \frac{1 - R_p^3}{3} \right. \right. \\ &\quad \left. \left. + \frac{3}{4} R_p^4 \ln R_p + \frac{3}{16}(1 - R_p^4) - \frac{1}{5} R_p^5 \ln R_p - \frac{1 - R_p^5}{25} \right) \right] \end{aligned} \tag{22}$$

where the interfacial velocity ratio to the bulk mean velocity (u_i / u_B) is already given by Equation (11) as a function of R_p and Da .

RESULTS AND DISCUSSION

The variations of Nusselt number are illustrated in Fig. (6a, b) where the Nusselt number is plotted against the porous core diameter ratio R_p . Upon changing the value of the diameter ratio R_p , analytical curves were generated using Equation (22) for a given set of the Darcy number and thermal conductivity ratio. Numerical computations were also carried out with $\epsilon=0.9$ for different Darcy numbers, namely, $Da=10^{-3}$, 10^{-4} and 10^{-5} . Both analytical and numerical sets of the results are compared with each other in Fig. (6a, b), for $k_e/k_f=1.4$ and 6, respectively, noting that the effective thermal conductivity is likely to be less than 10 for most porous media to be used for filling the core. Though the analytical results stay somewhat lower than the numerical results, the agreement between the two sets of the solutions appears to be fairly good over a wide range of R_p and Da . This proves the soundness of the present analytical treatment based on Darcy's law.

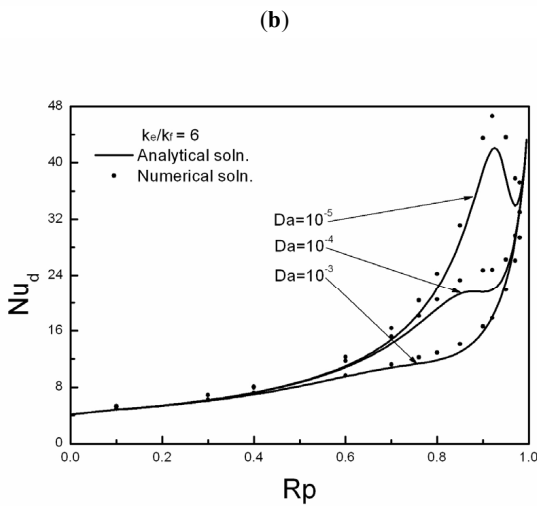
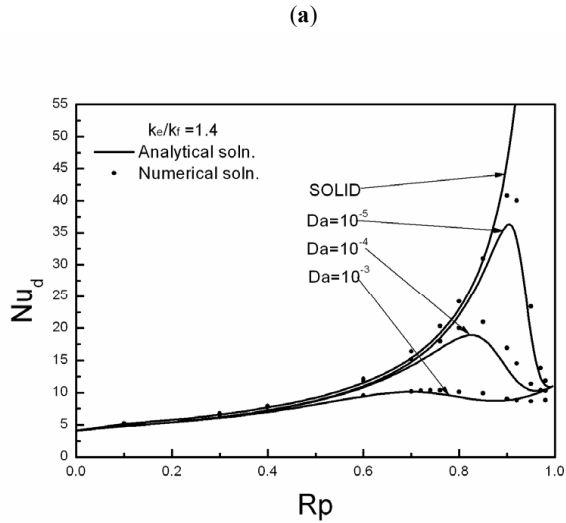


Fig. (6). The effects of R_p on the Nusselt number Nu_d (a) $k_e/k_f=1.4$ and $\epsilon=0.9$, (b) $k_e/k_f=6$ and $\epsilon=0.9$.

It is interesting to note that there exists the optimal porous core diameter ratio, which gives the local maximum Nusselt number. The presence of the porous core region guides the fluid particles towards the heated wall, such that the flow channeling takes place through the clear fluid annular region between the wall and the porous core interface. Thus, comparatively high velocity field is formed there, resulting the heat transfer enhancement from the wall to the fluid channeling through the annular region. However, as the pore core diameter increases further to make the annular gap between the wall and the interface of the porous medium small, the fluid particles come to experience higher flow resistance as channeling through the gap. In this way, the fluid particles passing through the small gap are blocked out. Finally, the fluid particles stay stagnant within the gap and thus find their way through the porous medium in the core region. This results in a drastic decrease in the Nusselt number, as can be seen from Fig. (6a, b).

As the figures show, the Nusselt number is higher for the lower Darcy number and its maximum value takes at the larger diameter ratio. The information on this optimal diameter ratio $(R_p)_{opt}$ yielding the maximum heat transfer coefficient may be quite useful for possible engineering applications such as designing effective heat transfer conduits. The analytical expression (22) is readily available for such a purpose to find $(R_p)_{opt}$ and the corresponding maximum Nusselt number. For the case of $k_e/k_f=1.4$, for example, the values of $(R_p)_{opt}$ may be correlated fairly well by:

$$(R_p)_{opt} = 1 - 1.73Da^{1/4} \text{ for } k_e/k_f=1.4 \tag{23}$$

Furthermore, the curve valid for the solid core, namely, $Da=0$, is generated and plotted in Fig. (6a), using the asymptotic expression reducible from Equation (22) for the case of $R_p \rightarrow 1$:

$$Nu_d = \frac{60}{13(1-R_p)} \text{ for } Da=0 \tag{24}$$

The foregoing equation appears to give fairly good approximations for the cases of comparatively large diameter ratio, say $R_p > 0.5$ when $Da=0$

As can be seen from both Fig. (6a, b), all curves for different Darcy numbers except for the solid core merge together at $R_p=1$. This value at $R_p=1$ can readily be found by carrying out an integration described in Equation (21) with $R_p \rightarrow 1$, which gives:

$$Nu_d = 8 \left(\frac{k_e}{k_f} \right) \text{ for } R_p=1 \tag{25}$$

irrespective of the value of Darcy number.

It should also be seen from Fig. (6b) that the Nusselt number for the case of large Darcy number exhibits its minimum value (lower than the value at $R_p=1$ given by Equation (25)), as increasing R_p towards 1. This undershooting of Nu_d results from the fact that the increase in the radial thermal conductivity due to the expansion of the porous medium region of high conductivity compensates and eventually overwhelms the convective heat transfer deterioration due to narrowing the gap. To the best of our knowledge, this undershooting phenomenon has not been inferred in the literature.

CONCLUSIONS

A theoretical treatment was presented to investigate fully developed forced convection in a tube with its core partially filled with a porous medium. Explicit expressions for the friction factor and Nusselt number for the case of constant heat flux were derived for possible engineering applications. It has been found that partial filling of the tube, up to a certain level of the porous core diameter, forms a high velocity field close to the wall working favorably to enhance heat transfer. However, any further increase beyond this level, results in the heat transfer deterioration since it tends to block the fluid particles channeling through the small gap formed between the wall and the porous core interface. A useful expression for the optimal porous core diameter ratio is presented as a function of the Darcy number. An experimental verification is underway, and will be reported in near future.

NOMENCLATURE

d	= Tube diameter
d_i	= Porous medium diameter
Da	= Darcy number
k	= Thermal conductivity
K	= Permeability
\dot{m}	= Mass flow rate
Nu_d	= Nusselt number
p	= Pressure
q_w	= Wall heat flux
u	= Axial velocity
r	= Cylindrical coordinate
Re_d	= Reynolds number
R_p	= Diameter ratio $R_p = d_i / d$

T	= Temperature
x	= Axial coordinate
ε	= Porosity
η	= Dimensionless radial coordinate $\eta = r / (d / 2)$
ρ	= Density
μ	= Viscosity
ν	= Kinematic viscosity
λ_f	= Friction factor

Subscripts

e	= Effective
f	= Fluid
i	= Interface

REFERENCES

- [1] A.V. Kuznetsov, "Analytical studies of forced convection in partly porous configurations", in: *Handbook of Porous Media*, K. Vafai, Ed. New York: Marcel Dekker, Inc., 2000, pp. 269-312.
- [2] D.A. Nield, and A. Bejan, *Convection in Porous Media*, 2nd ed. New York: Springer, 1999.
- [3] D.A. Nield and A.V. Kuznetsov, "Heat transfer in bidisperse porous media", in: *Transport Phenomena in Porous Media III*, D.B. Ingham and I. Pop, Eds. New York: Elsevier, 2005, pp. 34-59.
- [4] M. A. Al-Nir and M. K. Alkam, "Unsteady non-Darcian forced convection analysis in an annulus partially filled with a porous material", *ASME Trans. J. Heat Transfer*, vol. 119, pp. 799-804, 1997.
- [5] M. A. Al-Nir and M. K. Alkam, "Improving the performance of double-pipe heat exchanger by using porous substrates", *Int. J. Heat Mass Transfer*, vol. 42, pp. 3609-3618, 1999.
- [6] A. A. Mohamad, "Heat transfer enhancements in heat exchangers fitted with porous media, Part I: Constant wall temperature", *Int. J. Thermal Sci.*, vol. 42, pp. 385-395, 2003.
- [7] B. I. Pavel, and A. A. Mohamad, "An experimental and numerical study on heat transfer enhancement for gas heat exchangers fitted with porous media", *Int. J. Heat Mass Transfer*, pp. 4939-4952, 2004.
- [8] W. Liu, K. Yang, and A. Nakayama, "Enhancing heat transfer in the core flow by forming an equivalent thermal boundary layer in the fully developed tube flow", in *Proc. Sixth International Conference on Enhanced, Compact and Ultra-Compact Heat Exchangers: Science, Engineering and Technology*, 2007, pp. 245-250.
- [9] K. Vafai, and C. L. Tien, "Boundary and inertia effects on flow and heat transfer in porous media", *Int. J. Heat Mass Transfer*, vol. 24, pp. 195-203, 1981.
- [10] S. V. Patankar, *Numerical heat transfer and fluid flow*. Washington, DC: Hemisphere, 1980.
- [11] A. Nakayama, *PC-Aided numerical heat transfer and convective flow*. Boca Raton: CRC Press, 1995.
- [12] A. Nakayama, F. Kuwahara, T. Umamoto, and T. Hayashi, "Heat and fluid flow within an anisotropic porous medium", *ASME Trans. J. Heat Transfer*, vol. 124, pp. 746-753, 2002.